Performance Analysis of a TH-PPM UWB System using Dyadic Tree Structure

다이애딕 구조를 이용한 TH-PPM UWB 시스템의 성능 분석

박중후*, 최진규**

Joong-Hoo Park*, Ginkyu Choi**

Abstract

In this paper, certain scaling functions are generated using the dyadic subband tree structure and applied to a time-hopping, pulse position modulation, ultra-wideband (TH-PPM UWB) system. Scaling functions can be obtained by iterating a lowpass filter at each level using a critically sampled dyadic tree. The performance of the TH-PPM UWB system employing scaling functions as the mono-cycle waveform is evaluated through computer simulations in a Rayleigh fading environment.

Key Words : Scaling function, TH-PPM UWB system, Dyadic tree, Paraunitary Reconstruction

Ⅰ. Introduction

An ultra-wideband (UWB) system is emerging as a good candidate for next-generation radio systems because it is possible to share the existing radio spectrum and transmit high-rate data up to 200Mbps [1]. In a time-hopping, pulse position modulation, ultra-wideband (TH-PPM UWB) system, the Gaussian mono-cycle waveform is generally used for PPM modulation [2]. Recently, some researchers try to apply wavelet functions instead of Gaussian mono-cycle waveforms to UWB systems because UWB and wavelet signals share many positive properties such as high resolution and time and band-limited properties [3]. Both scaling and wavelet functions have been shown to be suitable for use in UWB communication [4]. A particular implementation of the Federal Communications Commission (FCC) compliant pulse generator using scaling functions for UWB systems in CMOS technology has also been presented in [5]. In this paper, scaling functions having similar properties are generated using the dyadic subband tree structure and applied to a TH-PPM UWB system. Scaling functions can be obtained by iterating a lowpass (LPF) filter at each level using a critically sampled dyadic

*정회원, 한양대학교 전자컴퓨터공학부
**정회원, 홍익대학교 전자전기공학과

tree. The TH-PPM UWB system employing scaling functions as the mono-cycle waveform is evaluated through computer simulations in a Rayleigh fading environment.

II. Generation of Scaling Functions

The dyadic subband tree structure is one choice among the hierarchical subband filter banks that provide multiresolution decomposition [6],[7]. It splits the frequency band into two equal bands at each level of the tree and then decomposes only one of these bands at the next level. This is called a critically sampled dyadic tree. Specially, three-level (or four-channel) dyadic tree is shown in Fig. 1.
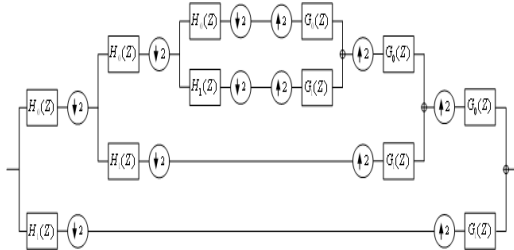

Figure 1. Dyadic tree structure.

It is now well understood [8] that a continuous scaling function can be obtained by iterating the LPF at each level using this dyadic tree.

It is shown that scaling functions have the following dilation property [6]

$$\phi(t) = \sqrt{2} \sum_{k=0}^{N-1} h[k]\phi(2t-k), \qquad (1)$$

where $h[k]$ is the LPF, N denotes the number of filter taps, the support of $\phi(t)$ is [0, N-1], and the completeness property of a multiresolution approximation implies that any scaling function has a non-zero DC gain, i.e., $\int_{-\infty}^{\infty} \phi(t)dt \neq 0$. Let $h_0[k]$ $h_1[k]$ be analysis filter, and $g_0[k]$ $g_1[k]$ the synthesis filter in the innermost two-band subband filter bank as in Figure. 1. Using the corresponding z transform, the choices

$$H_1(z) = z^{-(N-1)}H_0(-z^{-1}), G_0(z) = -H_1(-z),$$
$$G_1(z) = H_0(-z)$$
$$(2)$$

lead to paraunitary perfect reconstruction (PR) with the associated delay. The transfer function for these choices in the innermost two-band subband filter bank can be expressed as

$$H_0(z)H_0(z^{-1}) + H_0(-z)H_0(-z^{-1}) = 2. \quad (3)$$

In the time domain, we get

$$\sum_{k=0}^{N-1} h_0[k]h_0[k+2n] = \delta[n]. \qquad (4)$$

This condition satisfies the orthogonality to its integer shifts (translates), i.e.,

$$\int_{-\infty}^{\infty} \phi(t)\phi(t-n)dt = \delta[n]. \qquad (5)$$

Let $\Phi(\Omega)$ be the Fourier transform of $\phi(t)$ and define

$$H_0(\Omega) = \sum_{k=0}^{N-1} h_0[k]e^{-jk\Omega}. \qquad (6)$$

Then we obtain

$$\Phi(\Omega) = \frac{1}{\sqrt{2}}H_0(\frac{\Omega}{2})\Phi(\frac{\Omega}{2}), \quad (7)$$

or recursively

$$\Phi(\Omega) = \Phi(0)\prod_{k=1}^{\infty}\frac{1}{\sqrt{2}}H_0(\frac{\Omega}{2^k}). \quad (8)$$

This result implies

$$\sum_{k=0}^{N-1} h_0[k] = \sqrt{2}. \qquad (9)$$

Note that $N=4$ with the constraints of (4) and (9) gives one unconstrained filter coefficient. Among lots of choices the one filter coefficient which is robust for changes in input signal characteristics can be obtained in dyadic tree structure with embedded PDF-optimized quantizer as in Table 1 [7].
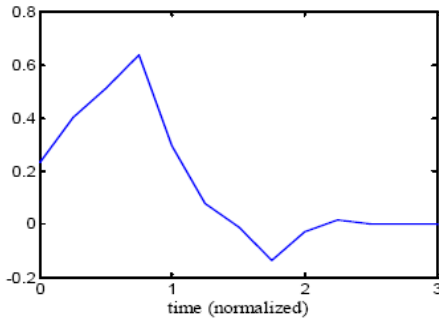

Figure 2. Scaling function

The values of coefficient are very slightly different from those as in [9] due to the constraints in dyadic tree structure: embedded

quantizer, average bit rate, compensation vector, input signal characteristics, no zero gain in the low pass filter, etc. This results in $\phi(t)$ using the fact that the infinite products as in (8) in the frequency domain are equivalent to infinite convolutions with the corresponding upsampled versions in the time domain as the following:

$$\phi(t) = \Phi(0)\frac{1}{\sqrt{2}}\sum_{k=0}^{N-1} h_0[k]\delta(2t-k)$$
$$* \frac{1}{\sqrt{2}}\sum_{k=0}^{N-1} h_0[k]\delta(4t-k) * \cdots.$$
$$(10)$$

where $*$ indicates convolution and $\Phi(0) = \int_{-\infty}^{\infty}\phi(t)dt \neq 0$. Figure. 2 shows $\phi(t)$ obtained by iterating only two times for the simplicity. This result shows that the scaling functions using dyadic tree can be generated based on the values of corresponding filter coefficient with some constraints. Note that the details of regularity or smoothness considerations resulting from (1) as in Figure. 2 are given in [9].

Table 1. $h_0[k]$

$h_0[0]$	$h_0[1]$	$h_0[2]$	$h_0[3]$
0.4829628	0.8365163	0.2241440	-0.1294096

III. A TH-PPM UWB System Employing Scaling Functions

In a TH-PPM UWB system, the transmitted signal for the kth user may be expressed as [10]

$$s^{(k)}(t) = \sum_{i=-\infty}^{\infty}\sqrt{P_k}w(t-iT_f-c_i^{(k)}T_c-b_{\lfloor i/N_s \rfloor}^{(k)}\Delta)$$
$$(11)$$

where P_k is the transmitted power, $w(t)$ is the mono-cycle waveform and normalized energy $\int_{-\infty}^{\infty} w^2(t)dt = 1$. Here, $w(t)$ is set to be $\phi(t)$ obtained in Section 2. The parameter T_f is the frame time, the sequence $c_i^{(k)}$ is the time-hopping code, T_c is the slot time, Δ is the pulse position offset, and N_s is the pulse repetition number. Finally, $b_{\lfloor i/N_s \rfloor}^{(k)}$ is information sequence taking on 0 or 1, and changes at multiples of N_s. Assuming that N_u users are transmitting on a L-path fading channel given by

$$h(t) = \sum_{l=0}^{L-1} \alpha_l \delta(t - \tau_l), \qquad (12)$$

the received signal can be expressed as

$$y(t) = h(t) * \sum_{k=0}^{N_u - 1} s^{(k)}(t) + n(t). \qquad (13)$$

In (12), α_l is the lth path gain coefficient and τ_l is the lth path delay time. The additive white Gaussian noise, $n(t)$, is assumed to be zero-mean with two-sided power spectral density of $N_0/2$. If maximal ratio combining is used in the correlator receiver, the receiver output for the interval $jT_f \le t < (j+1)T_f$ is given by

$$Z_j = \sum_{l=0}^{L-1} \alpha_l \int_{jT_f + \tau_l}^{(j+1)T_f + \tau_l} y(t)\nu(t - jT_f - \tau_l)dt. \qquad (14)$$

Here, the correlator template signal is $\nu(t) = w(t) - w(t - \Delta)$. An estimate of the desired user's information bit can be obtained as

$$\hat{b}_j = sgn(Z_j). \qquad (15)$$

IV. Simulation Results

In order to verify the TH-PPM UWB system employing a scaling funcation as the mono-cycle waveform, computer simulations have been performed in a Rayleigh fading environment. The performance of the system employing a scaling function is compared with the performance of the conventional system employing the Gaussian 2nd derivative function. To evaluate the BER performance, 100,000 data per user are transmitted over multi-path Rayleigh fading channels. The fading channel consists of two independent paths having equal power. The path delay of the second path varies from 0 to T_c. In Figures. 3-5, the BER performance of five-user TH-PPM UWB systems employing scaling functions are presented. In these cases, the spreading gain is set to be $N_s = 1, 2, 4$, respectively. To observe the intersymbol interference, the path delay of the second path was set to be $\tau = 0,\ 0.3\,T_c,\ 0.7\,T_c$. Figures. 3-5 show that the BER performance of the TH-PPM UWB system employing Gaussian function as a mono-cycle waveform degrades as the second path delay increases. But, the performance degradation is not observed for the TH-PPM UWB system employing scaling functions due to orthogonality condition at the given path delay. The simulation results show that the

intersymbol interference can be reduced effectively in the TH-PPM UWB system employing scaling functions.

Ⅴ. Conclusion

In this paper, scaling functions are generated using the dyadic subband tree structure and applied to a TH-PPM UWB system. Among lots of choices, the one filter coefficient which is robust for changes in input signal characteristics was used using dyadic tree structure with embedded PDF-optimized quantizer. The system performance was evaluated in a Rayleigh fading environment. The performance degradation was observed in the TH-PPM UWB system employing Gaussian function as a mono-cycle waveform. But, the performance degradation was not observed for the TH-PPM UWB system employing scaling functions due to orthogonality condition at the given path delay. This result shows another robustness of scaling function using the dyadic tree structure for the TH-PPM UWB system.
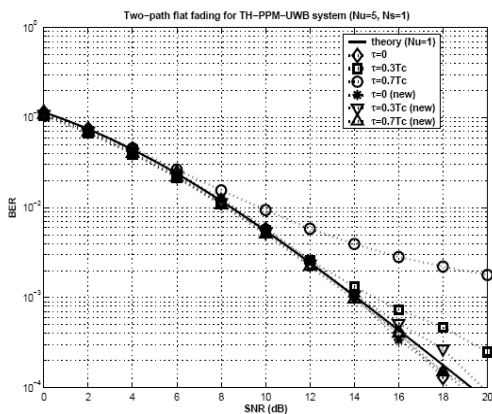
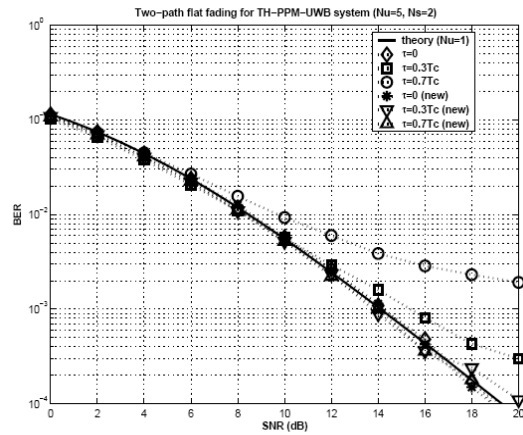Figure 3. Performance comparison of TH-PPM UWB systems $(N_s = 1)$

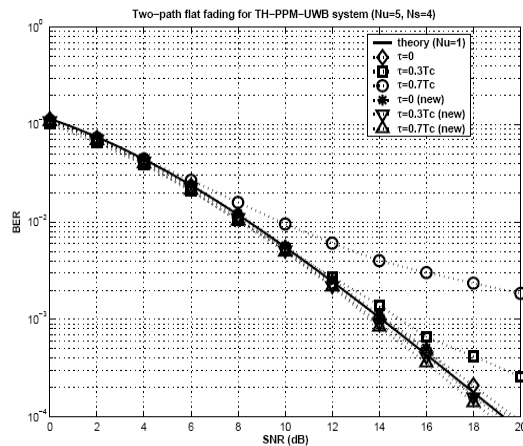Figure 4. Performance comparison of TH-PPM UWB systems $(N_s = 2)$

Figure 5. Performance comparison of TH-PPM UWB systems $(N_s = 4)$

References

[1] D. Porcino and W. Hirt, "Ultra-wideband radio technology: potential and challenges ahead," IEEE Commun. Mag., vol.41, no.7, pp.66-74, July 2003.
[2] W.M. Lovelace and J.K. Townsend, "The effects of timing jitter and tracking on the performance of impulse radio," IEEE Jourl. Selected Areas Commun., vol.20, no.9, pp. 1646-1651, December 2002.

[3] M.K. Lashmanan and H. Nikookar, "A Review of wavelets for digital wireless communication," Wireless Personal Communications: An International Jourl., vol.37, no.3-4, pp.387-420, May 2006.

[4] J.I. Agbinya and H.D. Truong, "A Comparison of ultra wideband signal functions for wireless adhoc networks," IEEE Third International Conference on Information Technology and Applications (ICITA), vol. 2, pp. 677-682, July 2005.

[5] S. Bagga, S.A.P. Haddad, W.A. Serdijn, and J.R. Long, "An FCC compliant pulse generator for IR-UWB communications," Proceedings of the IEEE International Symposium on Circuits and Systems (ISCAS), pp. 81-84, 2006.

[6] A.N. Akansu and R.A. Haddad, Multiresolution signal decomposition: transforms subbands wavelets, New York: Academic, 1992.

[7] G. Choi and R. A. Haddad, "Theory and design of dyadic subband tree with embedded PDF-optimized quantizers," IEEE Trans. Signal Processing, vol. 46, pp. 1260-1274, May 1998.

[8] P.P. Vaidyanathan, Multirate systems and filter banks, Englewood Cliffs, NJ: Prentice-Hall, 1993.

[9] I. Daubechies, Ten Lectures on wavelets, SIAM, Philadelphia, 1992.

[10] M.-G. Di Benedetto and G. Giancola, Understanding ultrawide band: radio fundamentals, Prentice-Hall, 2004.

───── 저 자 소 개 ─────

박중후(정회원)
• 1985년: 서울대학교 전자공학과 (BS),
• 1987년: 서울대학교 전자공학과 (MS),
• 1995년: (미) Univ. of Missouri-Rolla 전기공학과 (MS),
• 1997년: (미) Univ. of Missouri-Rolla 전기공학과 (Ph.D.),
• 1987년 ~ 1992년: LG 전자 수석연구원,
• 1992년 ~ 1993년: 나다텔 선임연구원,
• 1997년 ~ 2000년: 삼성전자 통신연구소 수석연구원,
• 2000년 ~ 현재 : 한양대학교 공학대 전자컴퓨터공학부 부교수
<관심분야: 디지털 통신, 이동 통신, OFDM 시스템, UWB 시스템>

최진규(정회원)
• 1983년: 성균관대학교 전자공학과 (BS),
• 1990년: (미)Polytechnic Univ. 전자전기공학과 (MS),
• 1994년: (미)Polytechnic Univ. 전산과학과 (MS),
• 1996년: (미)Polytechnic Univ. 전자전기공학과 (Ph.D),
• 1983년 ~ 1986년: LG 전자, Motolora Korea 연구원,
• 1996년 ~ 2004년: 삼성전자 통신연구소 수석연구원,
• 2004년 ~ 현재: 홍익대학교 과학기술대 전자전기공학과 조교수
<관심분야: 차세대이동통신, 초광대역 통신, 통신 신호처리>